IEEE Access
Multidisciplinary | Rapid Review | Open Access Journal

Received August 8, 2021, accepted August 23, 2021, date of publication August 26, 2021, date of current version September 8, 2021.

Digital Object Identifier 10.1109/ACCESS.2021.3108195

Multitarget Detection in Passive MIMO Radar Using Block Sparse Recovery

HOSSEIN NIKAEIN[1], ABBAS SHEIKHI[1], AND SAEED GAZOR[2], (Senior Member, IEEE)
[1]School of Electrical and Computer Engineering, Shiraz University, Shiraz 71348-51154, Iran
[2]Department of Electrical and Computer Engineering, Queen's University, Kingston, ON K7L 3N6, Canada

Corresponding author: Hossein Nikaein (hossein.nikaein@shirazu.ac.ir)

ABSTRACT In this paper, we develop a new algorithm for centralized target detection in passive MIMO radar (PMR) using sparse recovery technique. PMRs use a network of receivers and illuminators of opportunity to detect and localize targets. We consider a widely separated PMR network assuming the availability of reference channels. We first transform the collected information of all receivers to a common space and combine them to attain a unified model. The problem of target detection in the extracted model is equal to a block sparse recovery problem. Since employing the generic sparse recovery tools are impractical due to the ultra-large dimension of the sensing matrix, we exploit the structure of the involving matrices and propose a very efficient distributed algorithm which extracts all scatterers, including targets and clutter simultaneously with a unified procedure. The proposed algorithm is highly efficient, and it does not require a high bandwidth link to transfer raw data from nodes to the fusion center. Moreover, the algorithm inherently benefits from parallel processing and distributes the extensive computations among receivers. Our simulation results demonstrate that the proposed algorithm outperforms the popular PMR detection algorithm, especially in the presence of interfering targets and any strong clutter residue.

INDEX TERMS Passive coherent location, passive MIMO radar, block sparse recovery, radar multitarget detection.

I. INTRODUCTION

Passive radar as a sensor employs electromagnetic emission of existing transmitters to detect and localize targets. Some examples of these transmitters, which are called Illuminators of Opportunity (IOs), are digital audio broadcast (DAB) [1], Wi-Fi [2], and global system for mobile communications (GSM) [3]. Among various communication and broadcast transmitters, the FM radio [4] and digital video broadcasting–terrestrial (DVB-T) [5] are more popular IOs since they have widely spread stations with high power levels. Passive radars have gained a lot of attention recently. They are attractive as they do not need frequency allocation and do not interfere with wireless communication [6]. Furthermore, they can be inexpensive, reliable and can monitor the surrounding space without signature. We can design widely separated passive MIMO radar (PMR) by increasing the number of receivers and employed IOs, in order to achieve a significant diversity gain in the target detection and enhance localization accuracy. Such a system allows a target illuminated by multiple sources from different directions and at different frequencies and observed from different locations. Moreover, this gain resists to the target fading which has similar effect like spatial diversity in MIMO communication systems [7]. The PMR provides anti-stealth capability. Stealth targets are designed to diffuse their reflected energy in directions away from the direction of the impinging signals on them, in order to be hidden from the monostatic radars. Since receivers of a PMR are distributed in various directions, they enhance the chance to detect these reflections [8].

In passive bistatic radar, the conventional approach to detect targets and estimate their parameters is to use matched filtering of the received signal with transmitted waveform [1]. Since the transmitted waveform is a priori unknown, a reference channel (equipped with a high gain antenna steered toward the transmitter) is dedicated at each receiver to extract a clean copy of the transmitted waveform. The cross-ambiguity function (CAF) (between the outputs of the surveillance channel and the reference channel) is calculated and is compared with a threshold to detect targets.

The associate editor coordinating the review of this manuscript and approving it for publication was Davide Ramaccia.

Similar to active MIMO radar (AMR), centralized and decentralized approaches may be used for target detection and localization in PMR. In the decentralized approach, each of the bistatic (transmitter-receiver) pairs acts as an individual passive radar and detects targets independently. Then, they share and fuse their information across pairs by solving the intersections of bistatic ellipsoids to localize targets in a Cartesian space [9]. In the centralized approach, the received signals of all bistatic pairs are jointly processed, and target detection and localization are performed directly in Cartesian space. Hack *et al.* [10] showed that similar to AMR, the centralized approach outperforms the decentralized target detection.

Most existing studies on the centralized approach assume a PMR without using reference channels which is mainly the case of passive airborne radar, where the radar platform moves and prevents establishing a stationary direct-path between the transmitters and the receiver. In such a circumstance, the cross-correlation between the received signals of various receivers is used to detect and localize targets [11]. For example in [12], a multistatic passive radar was considered with a single transmitter and multiple receivers without reference channels. Then a signal model was formulated for a single target in the presence of noise with known variance and a generalized likelihood ratio test (GLRT) was derived for target detection. This problem was extended in [13] to the case of unknown noise power for which an GLRT-CFAR was derived. In these papers, it was assumed that the direct-path signal had been completely removed from the received signal. Unfortunately, this assumption is not realistic in practice and the direct-path is often a high power component of the received signal or may have residues [14]. As remedy in [15], a new GLRT is obtained by taking into account the direct-path.

In contrast to passive multistatic radar, most existing studies on the passive bistatic radar employ a reference channel which is assumed to provide an exact copy of the transmitted waveform [16], [17]. Analogously in this paper, we consider a PMR with distributed receivers which are equipped with reference channels. Furthermore, we assume that IOs transmit over a non-overlapping frequency spectrum. The authors in [10] considered the same assumptions and derived a GLRT for a single target in additive white Gaussian noise with known variance. As we will see in the simulation section, this extracted GLRT has very limitations, and when we have interfering targets with high SNR, it fails to detect the target properly and generate many false alarms. Based on this detector, another GLRT is derived in [18] for the same conditions but colored noise with unknown covariance matrix. In this GLRT, training samples are utilized to estimate covariance matrix of noise. In the extraction of these detectors, it is assumed that clutter and direct-path are entirely removed before target detection. Unfortunately, this is not always a realistic assumption [14], [19], and the high power of clutter and direct-path residue can cause excessive false alarms in the output.

To remedy these limitations, we use the sparsity of the radar scene and propose an algorithm for target detection employing sparse recovery tools in the Compressed Sensing (CS) framework. Recently, the CS has gained attention in various radar literature, such as in synthetic aperture radar [20], [21] Through-the-Wall Radar Imaging [22], and range-Doppler (RD) map generation [23]. In several papers, the CS and sparse recovery have been employed for signal processing in passive radars. A high-resolution algorithm in [24] is proposed to use sparse recovery for RD map generation. It reduces the sidelobes of the cross ambiguity function (CAF) by exploiting the sparsity of the scene in passive bistatic radars. In this method, the integration time is divided into multiple batches, and some of them are randomly selected to reduce computational complexity by using CS. For a multi-receiver Wi-Fi passive radar in [2], an off-grid sparse recovery algorithm is presented to achieve high resolution in localization. An algorithm is proposed in [17] for detection of targets using DAB as IO in a passive radar. This algorithm exploits the structure of the OFDM waveform and employs sparse recovery tools to yield a higher resolution in localization. A GLRT is proposed in [25] for a passive multistatic radar with one transmitter and multiple receivers without reference channels assuming that the IO waveform is sparse in the frequency domain. In [26], a CS approach is employed for the fusion of information collected from bistatic pairs of a passive multistatic radar. Such a CS framework is also used for MIMO radars in other works. For example in [27], a three-dimensional channel estimation algorithm is proposed by using the special structure of the OFDM waveform for an OFDM-based passive MIMO radar with co-located receivers. The estimator in [27] includes time delay, Doppler frequency, and angle of arrivals. The use of CS allows reducing the number of measurements of the observation matrix. In [28] a block sparse Bayesian learning method is used to localize targets in an active MIMO radar. In [29], an off-grid approach is employed to reduce the number of Grid Points (GPs) for a co-located MIMO radar. This approach allows to derive an accurate localization algorithm using target sparsity which is solved by a block sparse recovery method. The CS is used for target estimation in [30] for a widely separated active MIMO radar, where a low complexity algorithm is proposed for sparse recovery employing the alternating direction method of multipliers.

In this work, we propose a new algorithm for the detection of targets in PMR. We use a centralized approach to formulate the received signals for all bistatic pairs. Then we use the sparsity of the scene and propose to employ block sparse recovery tools to extract direct-path and all scatterers, including targets and clutter. The excessively large dimension of the sensing matrix demands an unacceptable computation complexity. Thus, we exploit the block-diagonal structure of the involving matrices and propose a computationally efficient algorithm with several orders of magnitude reduction in complexity. Distributed processing is an important advantage of the proposed algorithm. Furthermore, as the

main part of the algorithm is done locally in the receivers, we did not require high bandwidth links to transfer raw data from receivers to the fusion center (FC). In contrast to many passive radar methods, our proposed algorithm does not require the elimination of direct-path and clutter before target detection. It extracts all scatterers simultaneously in a unified procedure, and we can use post-processing algorithms to classify results. This method allows us to detect targets with small Doppler frequencies, whereas lower frequencies are usually eliminated in the interference cancellation part of the competing algorithms. Our simulation results demonstrate the superiority of the proposed algorithm over the popular PMR detection algorithms, especially in the presence of interfering targets and strong clutter.

The remainder of this paper is organized as follows. Section II presents a unified block-sparse model for received information at all bistatic pairs of a PMR. In Section III, we show that extracting targets is a block sparse recovery problem that requires an unacceptable order of computational complexity. As a remedy, we propose a very efficient distributed algorithm. We evaluate our proposed algorithm in Section IV via extensive simulation results. We finally draw conclusions in Section V.

II. REPRESENTATION OF RECEIVED INFORMATION

Consider a widely separated passive MIMO radar with M_t non-cooperative IOs and M_r receivers. This provides $M_t \times M_r$ bistatic radar pairs. We aim to detect targets in an FC by using these pairs. We assume that IOs transmit over non-overlapping frequencies, and receivers are equipped with filter banks separating their signals. We express N samples of the received signal $\mathbf{z}_{ij} \in \mathbb{C}^N$ from the output of the jth filter of ith receiver tuned at the frequency of the jth IO as follows [31]:

$$\mathbf{z}_{ij} = \mathbf{S}_{ij}\mathbf{a}_{ij} + \mathbf{n}_{ij} \quad 1 \le i \le M_r,\ 1 \le j \le M_t, \tag{1}$$

where $\mathbf{n}_{ij} \in \mathbb{C}^N$ is the additive white Gaussian noise, and the entries of $\mathbf{a}_{ij} = [a_{ij,1}, a_{ij,2}, \ldots, a_{ij,M}]^T$ are the complex amplitudes of either direct-path, targets returns, or clutter returns in the ijth bistatic pair. Each column of the $N \times M$ matrix $\mathbf{S}_{ij} \triangleq [\mathbf{s}_{1,ij}, \mathbf{s}_{2,ij}, \cdots, \mathbf{s}_{M,ij}]$, i.e., $\mathbf{s}_{m,ij}$ represents samples of returned signal from jth IO signal to ith receiver related to the mth scatterer. We can express it as follows

$$\mathbf{s}_{m,ij} = \mathbf{\Lambda}^{\Omega_m}\mathbf{P}^{n_m}\mathbf{s}_{ij}^R. \tag{2}$$

where $\mathbf{s}_{ij}^R$ is the received signal in the reference channel of ith receiver related to the jth transmitter and (n_m, Ω_m) is the pair of bistatic delay and Doppler frequency of mth scatterer. $\Lambda^{\Omega_m} = \mathrm{diag}(1, e^{j\Omega_m}, \cdots, e^{j(N-1)\Omega_m})$ is the Doppler shift operator with frequency Ω_m, and the $N \times N$ unit delay matrix $\mathbf{P}$ is defined by

$$[\mathbf{P}]_{i,j} = \begin{cases} 1 & i = j+1 \\ 0 & \text{otherwise,} \end{cases} \qquad i,j = 1,2,\ldots,N. \tag{3}$$

In order to detect targets, we need to determine M and estimate the set of dependent unknown parameters, i.e. $\{(n_m, \Omega_m)\}_{m=1,\cdots,M}$ and $\mathbf{a}_{ij}$ from (1). This nonlinear problem is NP-hard due to dependency of $\mathbf{s}_{m,ij}$ in (2) to the unknown parameters. As remedy, we propose to combine the information of all bistatic pairs in a common coordinate.

To make this solution more practical, we treat this problem as a network of $M_t \times M_r$ distributed sensors and deem the bistatic pairs as sensors. In the FC, we combine the data of these sensors in a Cartesian coordinate. For this fusion, we denote the location and velocity parameters of a target by triplets (x, y, z) and $(\dot{x}, \dot{y}, \dot{z})$, respectively. We propose to discretize the search space for (x, y, z) and $(\dot{x}, \dot{y}, \dot{z})$ respectively, with an expected range and velocity resolutions. This quantization of the search space creates a finite set of GPs [29]. A GP is a six-dimensional vector: $[x_k, y_k, z_k, \dot{x}_k, \dot{y}_k, \dot{z}_k]$ for $k = 1, \cdots, N_G$, where N_G is the total number of GPs. Let $[x_i^R, y_i^R, z_i^R]$ and $[x_j^T, y_j^T, z_j^T]$ denote the locations of ith receiver and jth transmitter, respectively. For a potential target in kth GP, the Doppler shift and delay for ijth bistatic pair are

$$\Omega_{ij,k} = \frac{f_j}{Cf_s}\Big(\frac{[\dot{x}_k, \dot{y}_k, \dot{z}_k]\delta_{i,k}^R}{\|\delta_{i,k}^R\|_2} + \frac{[\dot{x}_k, \dot{y}_k, \dot{z}_k]\delta_{j,k}^T}{\|\delta_{j,k}^T\|_2}\Big), \tag{4}$$

$$n_{ij,k} = \frac{f_s}{CT_s}\big(\|\delta_{i,k}^R\|_2 + \|\delta_{j,k}^T\|_2 - \|\delta_{i,j}^{RT}\|_2\big), \tag{5}$$

where C is the wave propagation speed, f_s is the sampling frequency, and f_j is the carrier frequency of jth IO signal and

$$\delta_{j,k}^T \triangleq \begin{bmatrix} x_k \\ y_k \\ z_k \end{bmatrix} - \begin{bmatrix} x_j^T \\ y_j^T \\ z_j^T \end{bmatrix}, \quad \delta_{i,k}^R \triangleq \begin{bmatrix} x_k \\ y_k \\ z_k \end{bmatrix} - \begin{bmatrix} x_i^R \\ y_i^R \\ z_i^R \end{bmatrix},$$
$$\delta_{i,j}^{RT} \triangleq \begin{bmatrix} x_i^R \\ y_i^R \\ z_i^R \end{bmatrix} - \begin{bmatrix} x_j^T \\ y_j^T \\ z_j^T \end{bmatrix}. \tag{6}$$

Now, we enlarge $\mathbf{S}_{ij}$ and $\mathbf{a}_{ij}$ in (1), to include reflected signals and related complex coefficients of all GPs. Thus, we rewrite (1) as follows

$$\mathbf{z}_{ij} = \mathbf{\Phi}_{ij}\mathbf{b}_{ij} + \mathbf{n}_{ij}, \quad 1 \le i \le M_r,\ 1 \le j \le M_t \tag{7}$$

where $\mathbf{\Phi}_{ij} \triangleq [\boldsymbol{\phi}_{ij,1}, \boldsymbol{\phi}_{ij,2}, \cdots, \boldsymbol{\phi}_{ij,N_G}] \in \mathbb{C}^{N \times N_G}$ and $\boldsymbol{\phi}_{ij,k} = \mathbf{\Lambda}^{\Omega_{ij,k}}\mathbf{P}^{n_{ij,k}}\mathbf{s}_{ij}^R$, also $(n_{ij,k}, \Omega_{ij,k})$ is the pair of bistatic delay and Doppler frequency of kth GP in ijth bistatic pair. Moreover, $\mathbf{b}_{ij} \in \mathbb{C}^{N_G}$ contains complex coefficients of reflected signals from GPs in ijth bistatic pair. We combine the information of all pairs in a single equation by concatenating $\mathbf{z}_{ij}$ in (7), which yields

$$\mathbf{z} = \mathbf{\Phi}\mathbf{b} + \mathbf{n}, \tag{8}$$

where

$$\mathbf{z} = \mathrm{vec}[\mathbf{z}_{11}, \cdots, \mathbf{z}_{M_tM_r}] \in \mathbb{C}^{M_tM_rN},$$
$$\mathbf{n} = \mathrm{vec}[\mathbf{n}_{11}, \cdots, \mathbf{n}_{M_tM_r}] \in \mathbb{C}^{M_tM_rN},$$

$$\begin{aligned}\boldsymbol{\Phi} &= \text{diag}(\boldsymbol{\Phi}_{11}, \ldots, \boldsymbol{\Phi}_{M_t M_r}) \in \mathbb{C}^{M_t M_r N \times M_t M_r N_G},\\ \mathbf{B} &= [\mathbf{b}_{11}, \cdots, \mathbf{b}_{M_t M_r}] \in \mathbb{C}^{N_G \times M_t M_r},\\ \mathbf{b} &= \text{vec}\mathbf{B} \in \mathbb{C}^{M_t M_r N_G}.\end{aligned} \tag{9}$$

Since $N \ll N_G$, the problem in (8) is heavily underdetermined. Thus we need a regularization constraint to solve it. We know that all entries of $\mathbf{b}_{ij}$s are zero except for GPs, which contain scatterer. Therefore, since the number of scatterers, i.e. M is much less than the number of GPs, $\mathbf{b}_{ij}$s are sparse vectors with the same sparsity pattern. This means only M rows of $\mathbf{B}$ are nonzero, and we may exploit this block sparsity constraint to solve $\mathbf{b}$ from (8) by using one of the existing block-sparse recovery algorithms. Unfortunately, the existing algorithms are impractical for this problem because of the enormous size of $\boldsymbol{\Phi}_{ij}$.

III. TARGET EXTRACTION VIA BLOCK SPARSE RECOVERY

In order to exploit the row sparsity of $\mathbf{B}$ in (8)-(9), we solve the following block sparse recovery problem

$$\min \sum_{k=1}^{N_G} \|\mathbf{b}_{\mathcal{G}_k}\|_2 \quad \text{s.t.} \quad \|\mathbf{z} - \boldsymbol{\Phi}\mathbf{b}\|_2 \leq \varepsilon, \tag{10}$$

where ε is a regulating parameter and the set $\mathcal{G}_k = \{p = tN_G + k | \forall t = 0, \cdots, M_t M_r - 1\}$ contains the indices of the unknown vector $\mathbf{b}$ which are related to kth GP. Thus, $\mathbf{b}_{\mathcal{G}_k}$ is the transpose of kth row of $\mathbf{B}$. It is ideal to minimize the number of nonzero values for $\|\mathbf{b}_{\mathcal{G}_k}\|_2$ instead of their ℓ_1-norm in (10). Unfortunately, the ideal ℓ_0-norm problem is NP-hard. Several algorithms in CS literature solve block sparse problems similar to (10), such as group Lasso [32], block version of OMP (BOMP) [33]–[35], and block- thresholding (BTH) algorithm [36]. Since the sensing matrix $\boldsymbol{\Phi}$ is ultra-large, we only consider the BOMP because of its lower computational complexity.

Algorithm 1 summarizes the BOMP procedure for solving (10). We initialize the residue vector $\mathbf{r}_l$ at $\mathbf{r}_0 = \mathbf{z}$ and start with an empty set for the selected GPs, i.e., $\mathcal{F} = \{\}$. Then in each iteration, we calculate the Euclidean norm of the correlation between the residue vector $\mathbf{r}_{l-1}$ and columns of $\boldsymbol{\Phi}_{\mathcal{G}_k}$ for $1 \leq k \leq N_G$. Where columns of $\boldsymbol{\Phi}_{\mathcal{G}_k}$ are the related columns of $\boldsymbol{\Phi}$ to kth GP, i.e.,

$$\boldsymbol{\Phi}_{\mathcal{G}_h} = \text{blockdiag}\left(\boldsymbol{\Phi}_{11,h}, \cdots, \boldsymbol{\Phi}_{M_t M_r,h}\right) \in \mathbb{C}^{NM_r M_t \times M_r M_t} \tag{11}$$

Then we select the GP with the maximum norm. We can write this procedure for the lth iteration as:

$$h_l = \underset{h \in \{1,\cdots,N_G\}}{\arg\max} \left\| \boldsymbol{\Phi}_{\mathcal{G}_h}^H \mathbf{r}_{l-1} \right\|_2^2 \tag{12}$$

Then, we append the selected GP h_l from (12) at lth iteration to $\mathcal{F}$, i.e., $\mathcal{F} \leftarrow \mathcal{F} \cup \{h_l\}$. We can now optimize $\mathbf{b}$ for $\mathcal{F}$ by solving the following problem:

$$\mathbf{b} = \underset{\mathbf{b}_{\mathcal{G}_k}: \forall k \in \mathcal{F}}{\arg\min} \| \mathbf{z} - \sum_{k \in \mathcal{F}} \boldsymbol{\Phi}_{\mathcal{G}_k}^H \mathbf{b}_{\mathcal{G}_k} \|_2. \tag{13}$$

We obviously have $\mathbf{b}_{\mathcal{G}_k} = 0$ for all $k \notin \mathcal{F}$. The solution of (13) is given by

$$\underline{\mathbf{b}}_{\mathcal{F}} = \left(\underline{\boldsymbol{\Phi}}_{\mathcal{F}}^H \underline{\boldsymbol{\Phi}}_{\mathcal{F}}\right)^{-1} \underline{\boldsymbol{\Phi}}_{\mathcal{F}}^H \mathbf{z}, \tag{14}$$

where the vector $\underline{\mathbf{b}}_{\mathcal{F}}$ and the matrix $\underline{\boldsymbol{\Phi}}_{\mathcal{F}}$ are obtained by concatenating the vectors $\mathbf{b}_{\mathcal{G}_k}$ and the matrices $\boldsymbol{\Phi}_{\mathcal{G}_k}$ for all $k \in \mathcal{F}$, respectively. We also update the residue $\mathbf{r}_l$ as follows

$$\mathbf{r}_l = \mathbf{z} - \sum_{k \in \mathcal{F}} \boldsymbol{\Phi}_{\mathcal{G}_k}^H \mathbf{b}_{\mathcal{G}_k}. \tag{15}$$

This BOMP procedure detects dominant scatterers one by one and eliminates their signatures in each iteration from $\mathbf{z}$ till a stopping criterion is reached, as summarized in Algorithm 1.

Algorithm 1 BOMP Algorithm for Target Detection in Passive MIMO Radar

1. Inputs: $\mathbf{z}$, $\boldsymbol{\Phi}$.
2. Initialize: $l \leftarrow 1$, $\mathbf{b} \leftarrow \mathbf{0}$, $\mathbf{r}_0 \leftarrow \mathbf{z}$, $\mathcal{F} \leftarrow \{\}$.
3. Repeat until stopping criterion is met:
4. $\quad h_l \leftarrow \underset{h \in \{1,\cdots,N_G\}}{\arg\max} \left\| \boldsymbol{\Phi}_{\mathcal{G}_h}^H \mathbf{r}_{l-1} \right\|_2^2$,
5. $\quad \mathcal{F} \leftarrow \mathcal{F} \cup \{h_l\}$.
6. $\quad \underline{\mathbf{b}}_{\mathcal{F}} \leftarrow \left(\underline{\boldsymbol{\Phi}}_{\mathcal{F}}^H \underline{\boldsymbol{\Phi}}_{\mathcal{F}}\right)^{-1} \underline{\boldsymbol{\Phi}}_{\mathcal{F}}^H \mathbf{z}$,
7. $\quad \mathbf{r}_l \leftarrow \mathbf{z} - \underline{\boldsymbol{\Phi}}_{\mathcal{F}} \underline{\mathbf{b}}_{\mathcal{F}}$
8. $\quad l \leftarrow l + 1$
9. Output: Sparse representation $\mathcal{F}$

A. DISTRIBUTED IMPLEMENTATION OF BOMP

The BOMP in Algorithm 1 has two main drawbacks. First, all received signals shall be transferred to the FC for each coherent processing time which requires a considerable communication bandwidth. Second, the extremely large dimensions of $\boldsymbol{\Phi}$ lead to an unbearable computational complexity.

To resolve these drawbacks, we propose to significantly lower the computational complexity and the amount of data transfer by exploiting the block-diagonal structure of $\boldsymbol{\Phi}$ in this problem. In particular, we propose to perform some of the computations at receivers and limit the amount of data transfers. In (14), the block diagonal matrix $\underline{\boldsymbol{\Phi}}_{\mathcal{F}}$ contains selected columns of $\boldsymbol{\Phi}$, i.e., we have

$$\underline{\boldsymbol{\Phi}}_{\mathcal{F}} = \text{diag}\left(\boldsymbol{\Phi}_{11,\mathcal{F}}, \cdots, \boldsymbol{\Phi}_{M_t M_r,\mathcal{F}}\right), \tag{16}$$

where the columns of $\boldsymbol{\Phi}_{ij,\mathcal{F}}$ are $\boldsymbol{\phi}_{ij,k}$ for all $k \in \mathcal{F}$. From the block diagonal structure of $\underline{\boldsymbol{\Phi}}_{\mathcal{F}}$ and the definitions of $\mathbf{z}$ and $\mathbf{b}$ in (9), we easily conclude that $\mathbf{b}_{ij,\mathcal{F}}$ can be calculated only by using $\boldsymbol{\Phi}_{ij,\mathcal{F}}$ and $\mathbf{z}_{ij}$. Therefor as in Step 6 of Algorithm 1, we compute (14) in parallel at ith receiver for all $i \in \{1, \cdots M_r\}, j \in \{1, \cdots, M_t\}$ as

$$\mathbf{b}_{ij,\mathcal{F}} = \left(\boldsymbol{\Phi}_{ij,\mathcal{F}}^H \boldsymbol{\Phi}_{ij,\mathcal{F}}\right)^{-1} \boldsymbol{\Phi}_{ij,\mathcal{F}}^H \mathbf{z}_{ij}, \quad \mathbf{b}_{ij,\mathcal{F}_l^c} = 0. \tag{17}$$

Moreover, we partition $\mathbf{r}$ into $M_t M_r$ vectors of equal length N, and break (15) (i.e., Step 7 of Algorithm 1) as follows in order to compute them in parallel at ith receiver

$$\mathbf{r}_{ij,l} = \mathbf{z}_{ij} - \mathbf{\Phi}_{ij,\mathcal{F}} \mathbf{b}_{ij,\mathcal{F}} \quad \forall j \in \{1, \cdots M_t\}. \tag{18}$$

Therefore by using (17) and (18), we can calculate $\mathbf{r}_{ij,l}$ and $\mathbf{b}_{ij,\mathcal{F}}$ locally at receivers in parallel. For these calculations, only $\mathcal{F}$ and $\mathbf{z}_{ij}$ are needed at ith receiver without transferring raw signals to the FC. However, we need to collect the residue vector $\mathbf{r}_{ij,l}$ from all bistatic pairs to select the next GP using (12). Therefore, the selection (12) shall be performed in one location, namely the FC. We assume that the FC broadcast the index of the selected GP, h_l, to all receivers using a feedback channel. From (11), we notice that $\mathbf{\Phi}_{\mathcal{G}_h}$ is a block diagonal matrix. Thus for all $h \in \{1, \cdots, N_G\}$, we have

$$\left\| \mathbf{\Phi}_{\mathcal{G}_h}^H \mathbf{r}_{l-1} \right\|_2^2 = \sum_{1 \le i \le M_r,\ 1 \le j \le M_t} \left| \mathbf{\Phi}_{ij,h}^H \mathbf{r}_{l-1,ij} \right|^2, \tag{19}$$

where ith receiver can locally calculate the term $\sum_{j=1}^{M_t} \left| \boldsymbol{\phi}_{ij,h}^H \mathbf{r}_{ij,l-1} \right|^2$ and transfer it to FC instead of $\mathbf{r}_{ij,l}$'s. These computed terms can be collectively compressed and transferred to the FC allowing to perform (12) using

$$h_l = \underset{h \in \{1,\cdots,N_G\}}{\arg\max} \sum_{i=1}^{M_r} \left(\sum_{j=1}^{M_t} \left| \mathbf{\Phi}_{ij,h}^H \mathbf{r}_{ij,l-1} \right|^2 \right). \tag{20}$$

This procedure allows converting Algorithm 1 to a distributed version as in Algorithm 2.

Algorithm 2 The Proposed Distributed BOMP Algorithm for Target Detection in Passive MIMO Radar

1. Inputs: $\mathbf{z}_{ij}$, $\mathbf{\Phi}_{ij}$ $1 \le i \le M_r$, $1 \le j \le M_t$
2. Initialize: $l \leftarrow 1$, $\mathbf{b}_{ij} \leftarrow \mathbf{0}$, $\mathbf{r}_{ij,0} \leftarrow \mathbf{z}_{ij}$, $\mathcal{F} \leftarrow \{\}$.
3. Repeat until stopping criterion is met:
4. $\quad h_l \leftarrow \underset{h \in \{1,\cdots,N_G\}}{\arg\max} \sum_{i=1}^{M_r} \left(\sum_{j=1}^{M_t} \left| \mathbf{\Phi}_{ij,h}^H \mathbf{r}_{ij,l-1} \right|^2 \right)$,
5. $\quad \mathcal{F} \leftarrow \mathcal{F} \cup \{h_l\}$.
6. $\quad$ for $i = 1 : M_r$ and $j = 1 : M_t$, do
7. $\quad\quad \mathbf{b}_{ij,\mathcal{F}} \leftarrow \left(\mathbf{\Phi}_{ij,\mathcal{F}}^H \mathbf{\Phi}_{ij,\mathcal{F}} \right)^{-1} \mathbf{\Phi}_{ij,\mathcal{F}}^H \mathbf{z}_{ij}$, $\mathbf{b}_{ij,\mathcal{F}^c} \leftarrow 0$
8. $\quad\quad \mathbf{r}_{ij,l} \leftarrow \mathbf{z}_{ij} - \mathbf{\Phi}_{ij,\mathcal{F}} \mathbf{b}_{ij,\mathcal{F}}$
9. $\quad$ end for
10. $\quad l \leftarrow l + 1$
11. Output: Sparse representation $\mathcal{F}$

In Algorithm 2, $\mathbf{r}_l$ and $\mathbf{b}$ are not calculated at the FC. Each receiver may calculate $\mathbf{b}_{ij}$ and $\mathbf{r}_{ij,l}$ and $\sum_{j=1}^{M_t} \left| \mathbf{\Phi}_{ij,h}^H r_{l-1,ij} \right|^2$ locally and instead shall only send the values of $\sum_{j=1}^{M_t} \left| \boldsymbol{\phi}_{ij,h}^H \mathbf{r}_{ij,l-1} \right|^2$ to the FC. The FC can add $\sum_{j=1}^{M_t} \left| \boldsymbol{\phi}_{ij,h}^H \mathbf{r}_{ij,l-1} \right|^2$ and selects the next GP h_l to maximize the sum of these values using (20) as in Step 4 of Algorithm 2. The matrix $\mathbf{\Phi}_{ij}$ has N_G columns which is a very large number. As a result, the calculation of correlation between its columns and $\mathbf{r}_{ij,l-1}$ demands a high computation power. Moreover, the transmission of the results to the FC requires high bandwidth. For example, using a passive radar employing a DVB-T signal and 0.1 second of integration time, we have $N \approx 10^6$. For a cube search space with dimensions of (20, 20, 5)Km and a lattice GP separation of 25m, we have $N_x N_y N_z = 800 \times 800 \times 200 = 1.2 \times 10^8$. In this example let the maximum target speed of this radar be 1Mach, and the velocity resolution be $3\frac{\mathrm{m}}{sec}$, which leads to $N_{v_x} N_{v_y} N_{v_z} = 100 \times 100 \times 100 = 10^6$ velocity instances. Accordingly, in this example, we have $N_G = N_x N_y N_z N_{v_x} N_{v_y} N_{v_z} = 1.2 \times 10^{14}$ GPs. Thus in this typical scenario, the matrix $\mathbf{\Phi}_{ij} \in \mathbb{C}^{10^6 \times 10^{14}}$ has ultra-large dimensions and cannot be stored or manipulated easily. In other words, it is impractical to calculate the correlation in (20). In summary, Algorithms 1 and 2 are mathematically equivalent and are both impractical for this application.

B. COMPUTATION OF CORRELATIONS OVER DELAY-DOPPLER SPACE

To overcome this challenge, we notice that many GPs have similar delay-Doppler for a given bistatic pair. Thus for each pair, we propose to calculate the correlation over delay-Doppler space first instead of GP space and transform the results to the GP space. For this purpose, we consider the maximum expected delay and Doppler in each bistatic pair and quantize them to delay-Doppler cells [31]. We define a matrix $\mathbf{\Psi}_{ij} \in \mathbb{C}^{N \times N_c}$ where N_c is the number of cells, and each column of $\mathbf{\Psi}_{ij}$ is a delayed and Doppler-shifted replica of the reference signal for a given delay-Doppler cell. The number of columns of $\mathbf{\Psi}_{ij}$ is considerably less than that of $\mathbf{\Phi}_{ij}$ as $N_c \ll N_G$. Therefore, we need significantly fewer computations to calculate the correlation between residue vector $\mathbf{r}_{ij,l-1}$ and columns of $\mathbf{\Psi}_{ij}$. For instance, in the above example, we have $\mathbf{\Psi}_{ij} \in \mathbb{C}^{10^6 \times 10^5}$, which reduces the number of required complex multiplications with an order of 10^9 for calculating the correlation. Moreover, we exploit the specific structure of $\mathbf{\Psi}_{ij}$ to further reduce the computational cost by using fast algorithms [37]. In particular, such a method utilizes FFT and does not require storing $\mathbf{\Psi}_{ij}$ in memory. After calculating the correlation in the delay-Doppler domain, we transform the results to the GPs domain. This transformation is a mapping between GPs and their related delay-Doppler cells and can be performed either at receivers or at the FC. It is easy to see that, we can substantially reduce the required communication bandwidth between receivers and the FC by performing these transformations at the FC. These modifications lead to our proposed algorithm for target detection in passive MIMO radar, which is implemented in parallel at sensors and the FC with reasonable computation and communication requirements. This algorithm is summarized in two parts, where Algorithm 3 and Algorithm 4 summarize the details executed at receivers and the FC, respectively.

Figure 1 shows the diagram of ith receiver of the proposed distributed algorithm, and Figure 2 shows the block diagram

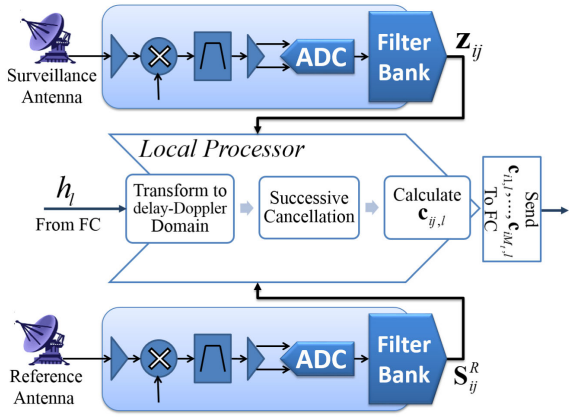

FIGURE 1. The block diagram of one of the receivers of the proposed algorithm.

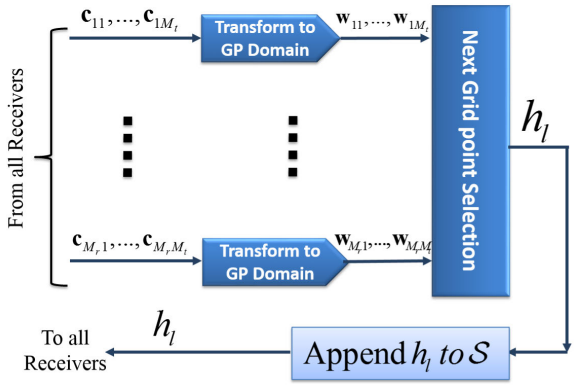

FIGURE 2. The block diagram of the FC part of the proposed algorithm.

Algorithm 3 The Portion of the Proposed Distributed Algorithm Executed at ith Receiver for All $j \in \{1, \cdots, M_t\}$

1. Inputs: $\mathbf{z}_{ij}$ and $\mathbf{s}_{ij}^R$.
2. Initialize: $l \leftarrow 1$, $\mathbf{a}_{ij} \leftarrow \mathbf{0}$, $\mathbf{r}_{ij,0} \leftarrow \mathbf{z}_{ij}$, $\mathcal{F} \leftarrow \{\}$.
3. Repeat until stopping criterion is met:
4. for $j = 1 : M_t$, do:
5. Calculate $\mathbf{c}_{ij,l} \leftarrow \mathbf{\Psi}_{ij}^H \mathbf{r}_{ij,l-1}$ using FFT,
6. end for
7. Send values of $[\mathbf{c}_{i1,l}, \cdots, \mathbf{c}_{iM_t,l}]$ to the FC.
8. Receive h_l from the FC.
9. for $j = 1 : M_t$, do:
10. Compute $(\Omega_{ij,h_l}, n_{ij,h_l})$ of h_l using (4)-(6) and append it to $\mathcal{I}_{ij}$.
11. $\mathbf{a}_{\mathcal{I}_{ij}} \leftarrow \left(\mathbf{\Psi}_{ij,\mathcal{I}_{ij}}^H \mathbf{\Psi}_{ij,\mathcal{I}_{ij}}\right)^{-1} \mathbf{\Psi}_{ij,\mathcal{I}_{ij}}^H \mathbf{z}_{ij}$, $\mathbf{a}_{ij,\mathcal{I}_{ij}^c} \leftarrow 0$,
12. $\mathbf{r}_{ij,l} \leftarrow \mathbf{z}_{ij} - \mathbf{\Psi}_{ij,\mathcal{I}_{ij}} \mathbf{a}_{\mathcal{I}_{ij}}$,
13. end for
14. $l \leftarrow l + 1$

of FC. In lth iteration of Algorithms 3, we first calculate 2D cross-correlation function $\mathbf{c}_{ij,l} = \mathbf{\Psi}_{ij}^H \mathbf{r}_{ij,l-1} \in \mathbb{C}^{N_c \times 1}$ for all bistatic pairs. Then, entries of $[\mathbf{c}_{i1,l}, \cdots, \mathbf{c}_{iM_t,l}]$ are sent to the FC (see Steps 4-7 of Algorithm 3). The FC receives

Algorithm 4 The Portion of the Proposed Distributed Algorithm Executed at the FC

1. Initialize: $l \leftarrow 1$
2. Repeat until stopping criterion is met:
3. for $i = 1 : M_r$, do
4. Receive $[\mathbf{c}_{i1,l}, \cdots, \mathbf{c}_{iM_t,l}]$ from ith receiver,
5. for $j = 1 : M_t$, do
6. transform $\mathbf{c}_{ij,l}$ to GPs domain, i.e., $\mathbf{w}_{ij,l}$,
7. end for
8. end for
9. Select $h_l \leftarrow \underset{h \in \{1,\cdots,N_G\}}{\arg\max} \sum_{\substack{1 \le i \le M_r \\ 1 \le j \le M_t}} \left|[\mathbf{w}_{ij,l}]_h\right|^2$, and
$$\mathcal{E}_l \leftarrow \max_{h \in \{1,\cdots,N_G\}} \sum_{\substack{1 \le i \le M_r \\ 1 \le j \le M_t}} \left|[\mathbf{w}_{ij,l}]_h\right|^2,$$
10. Broadcast h_l to all receivers,
11. $\mathcal{S} \leftarrow \mathcal{S} \cup \{(h_l, \mathcal{E}_l)\}$.
12. $l \leftarrow l + 1$
13. Output: Detected scatterers and their energy $\mathcal{S}$

$[\mathbf{c}_{i1,l}, \cdots, \mathbf{c}_{iM_t,l}]$ from all receivers and transforms them to $\mathbf{w}_{ij,l} \in \mathbb{C}^{1 \times N_G}$ to represent the GPs domain (see Steps 4-7 of Algorithm 4). Then using $\mathbf{w}_{ij,l}$ at the FC, we can compute (20) in order to select the next GP as in Step 9 of Algorithm 4. The index of selected GP, h_l, is broadcasted to all receivers as Step 10 of Algorithm 4. Then, it is appended to $\mathcal{S}$ accompany with its energy, i.e., $\mathcal{E}_l$. We compare $\frac{\mathcal{E}_l}{\|\mathbf{r}_{l-1}\|_2^2}$ with a threshold as a stopping criterion. In receivers, this newly selected point is transformed to the delay-Doppler domain for each pair, and appended to the set of selected cells, i.e. $\mathcal{I}_{ij}$ (see Step 10 of Algorithm 3). The set $\mathcal{I}_{ij}$ represents $\mathcal{F}$ and contains the selected pairs of delay-Doppler for ijth bistatic pair. Then in Steps 13 and 14, the relevant signals of these delay-Doppler cells, i.e. $\mathbf{\Psi}_{ij,\mathcal{I}_{ij}}$ are eliminated from observation vector $\mathbf{z}_{ij}$, and the new residue vector $\mathbf{r}_{ij,l}$ is generated. Furthermore, the vector $\mathbf{a}_{ij}$, which contains the complex coefficients of all delay-Doppler cells in ijth bistatic pair, are updated. This algorithm yields similar results as Algorithm 1 while it has several orders of magnitude less computation complexity. Moreover, in this method, we do not need to transfer raw signals (i.e., $\mathbf{z}_{ij} \in \mathbb{C}^N$, $\mathbf{s}_{ij}^R \in \mathbb{C}^N$) from receivers to the FC; instead, we only need to send the dominant entries of $\mathbf{c}_{ij,l} \in \mathbb{C}^{N_c}$, which yields less bandwidth requirement between receivers and the FC. Furthermore, the main parts of computations are distributed among all receivers, and we can use parallel processing substantially.

IV. SIMULATION RESULTS

In this section, we use numerical simulations to illustrate the performance of the proposed algorithm in target detection for a passive MIMO radar with two transmitters and three receivers. We consider DVB-T transmitters with 7.61MHz bandwidth, 9.14MHz sampling frequency, 8K mode, and cyclic prefix ratio of $\frac{1}{8}$. Transmitters carrier frequencies are 600MHz and 610MHz, and we choose an integration time of 28ms. In this simulation, we consider two scenarios.

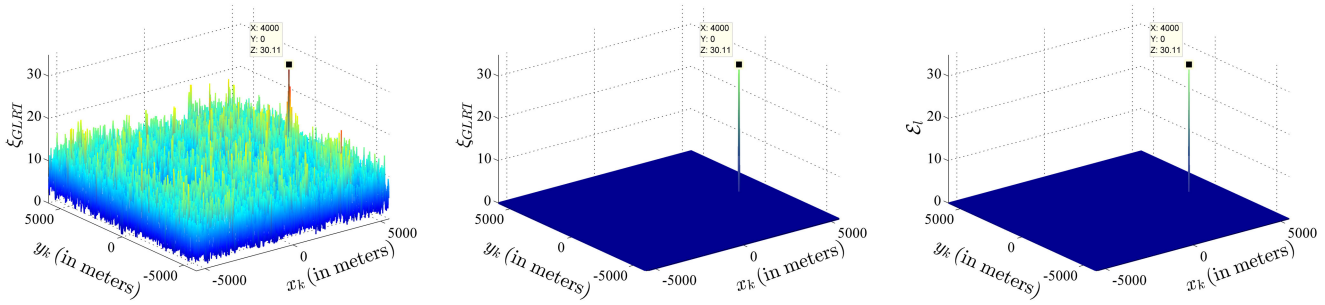

(a) Test statistic of AMR-GLRT. (b) Output of AMR-GLRT. (c) Output of the proposed algorithm.

FIGURE 3. Test statistic and output of AMR-GLRT and proposed algorithms in the single-target scenario with SNR = −49dB.

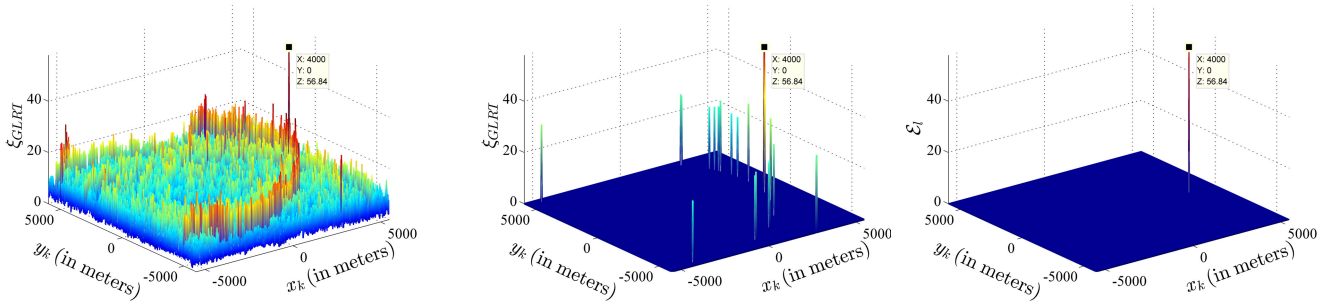

(a) Test statistic of AMR-GLRT. (b) Output of AMR-GLRT. (c) Output of the proposed algorithm.

FIGURE 4. Test statistic and output of AMR-GLRT and proposed algorithms in the single-target scenario with SNR = −44dB.

TABLE 1. 2D coordinate (in meters) of 2 transmitters, 3 receivers and 3 targets for simulation setup.

	Transmitter		Receiver			Target		
	#1	#2	#1	#2	#3	#1	#2	#3
x	500	-500	-4000	-4000	-4000	4000	3100	1000
y	4000	-4000	2000	500	-2500	0	2000	-3000

The first scenario consists of a single-target in the presence of Gaussian noise. The second scenario includes multiple targets and clutter. In order to reduce the computation time of simulation in our assessment and simplify our illustrations, we perform our simulations over a 2-D plane and assume all targets are stationary. The locations of transmitters, receivers, and targets are given in Table 1. The search space of radar covers a rectangle $x \in [-5500, 5500]$ and $y \in [-6000, 6000]$ in meters. We quantize this space into a rectangular lattice with 25 m distance between GPs.

As we noted in Section I, only a small number of papers (see [10] and references therein) have considered PMR with the existence of reference channels. The authors in [10] derived two GLRT detectors for PMR and AMR, namely PMR-GLRT and AMR-GLRT respectively. They showed that the performance of the PMR-GLRT tends the performance of the AMR-GLRT as the reference DNR increases (this appears as an upper bound for that of the PMR-GLRT). Therefore, we compare our proposed method with the AMR-GLRT as a benchmark. The AMR-GLRT uses a matched filter for each GP in all bistatic pairs. Then, the output of these matched filters are integrated non-coherently to calculate a test statistic as follows [10]:

$$\xi_{GLRT} = \frac{1}{\sigma^2} \sum_{i=1}^{M_r} \sum_{j=1}^{M_t} \left| \tilde{S}_{ij,h}^H \mathbf{z}_{ij} \right|^2 \underset{H_0}{\overset{H_1}{\gtrless}} \eta, \quad 1 \le h \le N_G \quad (21)$$

where $\tilde{S}_{ij,h}$ is defined in [10] as ijth reference signal whose delay and Doppler are compensated for hth GP, and σ is the noise variance. For simplicity in our simulations, we assume that all targets are observed with identical input signal-to-noise ratios (SNRs) at all bistatic pairs, which are defined by $\text{SNR}_i = \frac{|\alpha_m|^2}{\sigma^2}$, where α_m is the amplitude of received signal related to mth target.

We first evaluate the single-target scenario with transmitters, receivers, and target T_1 in Table 1. We consider an input SNR of −49dB for target T_1 at all bistatic pairs. Fig. 3a shows the test statistic of AMR-GLRT for all GPs in the search space of radar, and Fig. 3b shows detected targets after applying a threshold by using cell-average constant false alarm rate (CA-CFAR) [38] to this test statistic. Furthermore, Fig. 3c shows the output of our proposed algorithm using only one iteration. We observe that both methods properly detect T_1 without any false target.

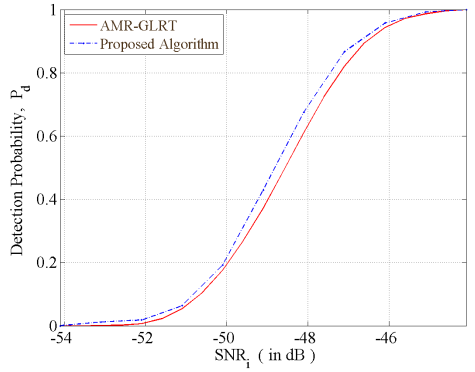

(a) P_{d} versus SNR$_i$

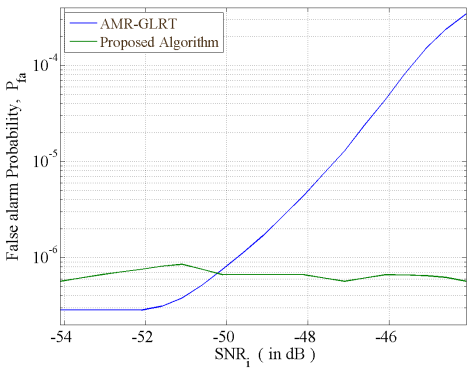

(b) P_{fa} versus SNR$_i$

FIGURE 5. Detection performance comparison of AMR-GLRT and proposed algorithm in the single-target scenario.

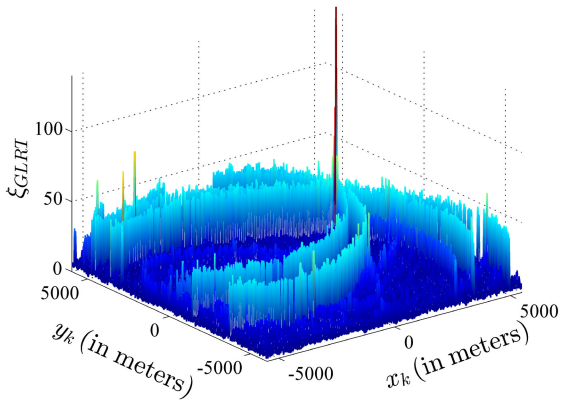

FIGURE 6. Test statistic of AMR-GLRT in the multitarget scenario.

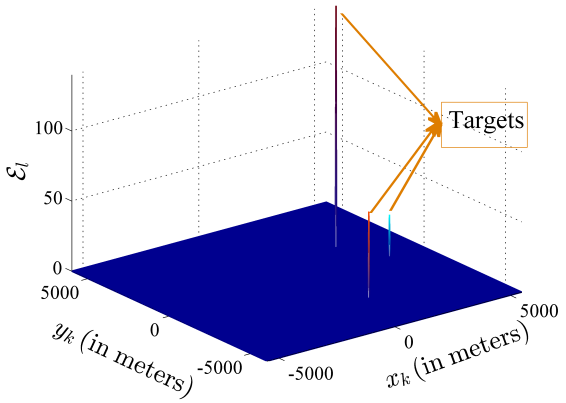

FIGURE 7. Detected scatterers in the output of the proposed algorithm in the simulated multitarget scenario.

Fig. 4a shows the test statistic of AMR-GLRT for all GPs for an increased input SNR at −44dB. We visibly observe the constant bistatic range ellipses in Fig. 4a generated by target T_1 at various bistatic pairs. These ellipses intersect in the location of target T_1. They have high-level sidelobes, which cause many false targets after applying of CA-CFAR threshold. These false targets are shown in Fig. 4b, which indicates an increase of a target SNR causes an increase of false targets in AMR-GLRT. In contrast to it, Fig. 4c shows that our proposed algorithm detects T_1 without the generation of any false target. Now we compare the performance of AMR-GLRT with the proposed algorithm more precisely. For this purpose, we set the detection threshold of both algorithms to attain $P_{\mathrm{fa}} = 10^{-6}$ for noise-only conditions. Then we change the input SNR (SNR$_i$) of T_1 and depict the detection probability P_{d} versus SNR$_i$ for both algorithms in Fig. 5a. We count the number of extra detected targets and divide it by number of grid points and average the results over the number of experiments in order to calculate the false alarm probability P_{fa} versus SNR$_i$ as plotted in Fig. 5b. This figure shows that the detection performance of these algorithms are similar, whereas the P_{fa} of AMR-GLRT increases rapidly when the target SNR increases.

Now, we consider a scenario with multiple targets to evaluate the performance of the proposed algorithm in real situations. In this scenario, three targets, as listed in Table 1 are places in the search region of radar. The input SNR for target T_1, T_2, and T_3 is equal to −51dB, −39dB and −44dB, respectively. Fig. 6 shows the resulted test statistic of AMR-GLRT for all GPs in this scenario. We observe that the constant bistatic range ellipses related to target T_2 cover many of GPs. That is because of its high SNR. Therefore, we cannot expect easy detection of other targets. Applying an adaptive threshold based on CA-CFAR to this test statistic causes a large number of false targets. However, as seen in Fig. 7, our proposed algorithm extracts all three targets without any false target.

Now, we evaluate the detection probability of AMR-GLRT and proposed algorithm algorithms in this scenario to compare them quantitatively. In this procedure, we keep the T_2 SNR and T_3 SNR as before and change the SNR of T_1 and depict P_{d} versus it. Fig. 8 shows the result of this test. As it can be seen, our proposed algorithm has a higher detection probability compare to AMR-GLRT. Furthermore, the P_{fa} of our algorithm remains unchanged and is about 10^{-6}, which is set in noise-only conditions. At the same time, the P_{fa} of AMR-GLRT is more than 10^{-2} for all SNR values of T_1.

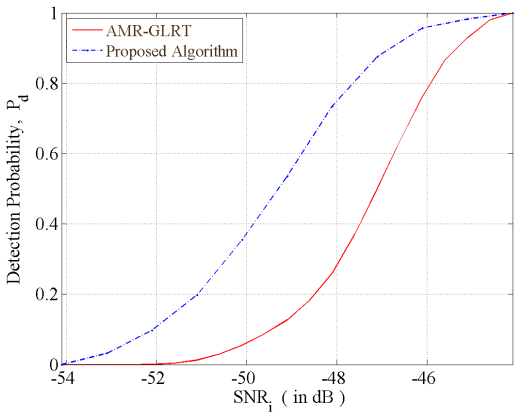

FIGURE 8. Detection performance comparison of AMR-GLRT and proposed algorithm in the multitarget scenario.

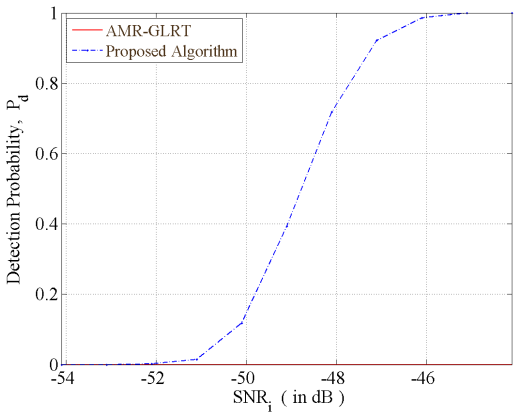

FIGURE 10. Detection performance comparison of AMR-GLRT and proposed algorithm in the presence of strong clutter and direct-path.

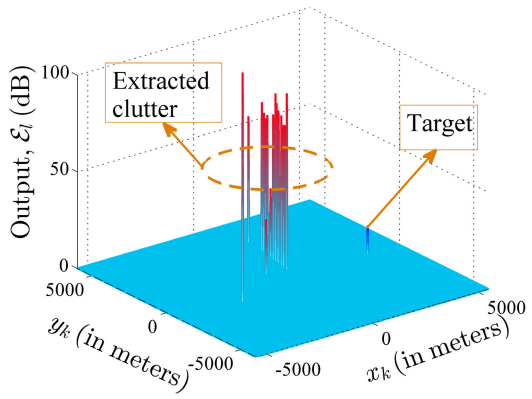

FIGURE 9. Detection of target T_1 in the presence of strong clutter and direct-path in the output of the proposed algorithm.

The results of these simulations show that AMR-GLRT can work properly in the single-target situation with low SNR targets. However, it causes extra false alarms in multitarget situations with high SNR targets. The same condition can occur when direct path or clutter have not been removed entirely before applying AMR-GLRT. In real situations, clutter return and direct path cannot be omitted completely by interference cancellation algorithms [19]. Therefore, the high power residue of clutter or direct path can cause the failure of AMR-GLRT.

Now, we illustrate the detection capability of our proposed algorithm in the presence of interference. We consider the previous single-target scenario and add heavy clutter and high power direct-path to the input signal of bistatic pairs. In this simulation, we consider a direct-path with a direct-to-noise ratio DNR_i of 60dB. Also, the variance of clutter amplitude is based on clutter to noise ratio CNR_i of 30dB. Fig. 9 shows the output of the proposed algorithm in this simulation. As it is seen, our proposed algorithm simultaneously extracts direct-path, clutter, and target with a unified procedure without any prior knowledge about the location or statistics of clutter. Therefore we can use post-processing algorithms (such as clutter map) to classify extracted scatterers. This method prevents eliminating of targets with low Doppler frequency. Now, we evaluate the performance of the proposed algorithm more precisely. For this purpose, we depict the P_{d} versus SNR_i for AMR-GLRT and our proposed algorithm in this scenario in Fig. 10. As it can be seen, AMR-GLRT completely fails to detect target. However, We observe that the detection performance of our proposed algorithm is very close to Fig. 5, where there is no clutter or direct path. This means that proposed algorithm can easily detect targets in the presence of strong clutter and direct-path.

Finally, we would like to investigate the computational complexity of the proposed algorithm in terms of the number of complex multiplications (CMs) and compare it with AMR-GLRT. We show the total number of CMs for AMR-GLRT with $\mathcal{C}_{AMR-GLRT}$, and for the proposed algorithm with $\mathcal{C}_{Proposed}$. In each iteration of Algorithm 3, Step 5 is related to the calculation of the correlation between residue vector $\mathbf{r}_{ij,l-1}$ and columns of $\mathbf{\Psi}_{ij}$ for the ijth bistatic pair. Then in Step 6 of Algorithm 4, these correlation is transformed to the domain of GPs, and in Step 9 of this algorithm, they are integrated non coherently for all GPs. This procedure is equal to the calculation of test statistics for all GPs in AMR-GLRT, and has the same complexity. We can use the Fourier transform FFT approach in [37] to calculate correlations in (21), which needs $N[1+\log_2(N)]N_{bin}$ CMs for each bistatic pair, where N_{bin} is the total number of range bins. Thus the total number of CMs for calculating AMR-GLRT is approximately $M_t M_r \log_2(N) N N_{bin}$, i.e.

$$\mathcal{C}_{AMR-GLRT} \approx M_t M_r N \log_2(N) N_{bin}. \tag{22}$$

In Step 10 of Algorithm 4, the selected GP is transferred to receivers, and in Step 11 and 12 of Algorithm 3 its related signal is removed from the received signal in all bistatic pairs based on a least-square calculation. Since in the lth iteration, the size of $\mathbf{\Psi}_{ij,\mathcal{I}_{ij}}$ is equal to $N \times l$, the number of CMs for implementation of Steps 11 and 12 is equal

to $\left(Nl^2 + 2\,Nl + l^3 + l^2 + N\right)$. Now by considering that $l \ll N$, the total number of CMs for all bistatic pairs in these steps is approximately equal to $M_t M_r N l^2$ in the lth iteration. Consequently, the total CMs for our proposed algorithm in the lth iteration is equal to $\mathcal{C}_{AMR-GLRT} + M_t M_r N l^2$. If we define the L as the number of all detected scatterers, including targets and residue of clutter, the number of iteration will be equal to L, and we have

$$\mathcal{C}_{Proposed} \approx L\mathcal{C}_{AMR-GLRT} + 2L^3 M_t M_r N/3. \tag{23}$$

As many of range bins do not have any scatterers, we can suppose $L^2 \ll \log_2(N)N_{bin}$, and we can ignore the second term in (23). Accordingly, the computation complexity of the proposed algorithm is in the order of L times of AMR-GLRT. This increase in the computation complexity provides an essential improvement in the target detection in real situations with multiple targets and strong clutter plus direct-path.

V. CONCLUSION

In this work, we considered a PMR with the existence of reference channels. Then to detect and localize targets by a centralized approach, we transformed the collected information of all bistatic pairs to a common space and fused them to attain a unified model. The problem of target detection in the extracted model is equal to a block sparse recovery problem. Due to the ultra-large dimension of the sensing matrix, we could not use popular sparse recovery tools such as BOMP for this problem. Therefore we employed the particular structure of our model and proposed a very efficient algorithm with significantly fewer computations and memory requirements than BOMP. Our proposed algorithm does not require a high bandwidth link between the FC and receiver to transfer raw data. Additionally, it can be distributed among receivers and benefit from parallel processing. Our proposed algorithm does not require removing clutter and other interference before target detection. It extracts all scatterers including targets and clutter, simultaneously with a unified procedure. Provided simulation results, demonstrated that the proposed algorithm outperforms the previous popular GLRT based PMR detection algorithm, especially in the presence of interfering targets and strong clutter residue.

REFERENCES

[1] M. Weiss, "Compressive sensing for passive surveillance radar using DAB signals," in *Proc. Int. Radar Conf.*, Oct. 2014, pp. 1–6.

[2] J. Wu, Y. Lu, and W. Dai, "Off-grid compressed sensing for WiFi-based passive radar," in *Proc. IEEE Int. Symp. Signal Process. Inf. Technol. (ISSPIT)*, Dec. 2016, pp. 258–262.

[3] P. Krysik, P. Samczynski, M. Malanowski, L. Maslikowski, and K. S. Kulpa, "Velocity measurement and traffic monitoring using a GSM passive radar demonstrator," *IEEE Aerosp. Electron. Syst. Mag.*, vol. 27, no. 10, pp. 43–51, Oct. 2012.

[4] M. Malanowski, K. Kulpa, J. Kulpa, P. Samczynski, and J. Misiurewicz, "Analysis of detection range of FM-based passive radar," *IET Radar, Navigat.*, vol. 8, no. 2, pp. 153–159, Feb. 2014.

[5] W. Feng, J.-M. Friedt, S. Wang, H. Liu, and M. Sato, "Passive bistatic radar using digital terrestrial television broadcasting signal for subsurface target detection," in *Proc. Photon. Electromagn. Res. Symp. Fall (PIERS–Fall)*, Dec. 2019, pp. 586–597.

[6] H. Kuschel, D. Cristallini, and K. E. Olsen, "Tutorial: Passive radar tutorial," *IEEE Aerosp. Electron. Syst. Mag.*, vol. 34, no. 2, pp. 2–19, Feb. 2019.

[7] E. Fishler, A. Haimovich, R. Blum, L. Cimini, D. Chizhik, and R. Valenzuela, "Spatial diversity in radars—Models and detection performance," *IEEE Trans. Signal Process.*, vol. 54, no. 3, pp. 823–838, Mar. 2006.

[8] H. Griffiths, "Multistatic, MIMO and networked radar: The future of radar sensors," in *Proc. 7th Eur. Radar Conf.*, Sep. 2010, pp. 81–84.

[9] M. Malanowski and K. Kulpa, "Two methods for target localization in multistatic passive radar," *IEEE Trans. Aerosp. Electron. Syst.*, vol. 48, no. 1, pp. 572–580, Jan. 2012.

[10] D. E. Hack, L. K. Patton, B. Himed, and M. A. Saville, "Detection in passive MIMO radar networks," *IEEE Trans. Signal Process.*, vol. 62, no. 11, pp. 2999–3012, Jun. 2014.

[11] Z. Geng, "Evolution of netted radar systems," *IEEE Access*, vol. 8, pp. 124961–124977, 2020.

[12] K. S. Bialkowski, I. V. L. Clarkson, and S. D. Howard, "Generalized canonical correlation for passive multistatic radar detection," in *Proc. IEEE Stat. Signal Process. Workshop (SSP)*, Jun. 2011, pp. 417–420.

[13] J. Liu, H. Li, and B. Himed, "Two target detection algorithms for passive multistatic radar," *IEEE Trans. Signal Process.*, vol. 62, no. 22, pp. 5930–5939, Nov. 2014.

[14] R. Tao, H. Wu, and T. Shan, "Direct-path suppression by spatial filtering in digital television terrestrial broadcasting-based passive radar," *IET Radar, Sonar Navigat.*, vol. 4, no. 6, pp. 791–805, Jan. 2011.

[15] X. Zhang, H. Li, and B. Himed, "A direct-path interference resistant passive detector," *IEEE Signal Process. Lett.*, vol. 24, no. 6, pp. 818–822, Jun. 2017.

[16] F. Colone, D. W. O'Hagan, P. Lombardo, and C. J. Baker, "A multistage processing algorithm for disturbance removal and target detection in passive bistatic radar," *IEEE Trans. Aerosp. Electron. Syst.*, vol. 45, no. 2, pp. 698–722, Apr. 2009.

[17] C. R. Berger, B. Demissie, J. Heckenbach, P. Willett, and S. Zhou, "Signal processing for passive radar using OFDM waveforms," *IEEE J. Sel. Topics Signal Process.*, vol. 4, no. 1, pp. 226–238, Feb. 2010.

[18] Y. Liu, G. Liao, H. Li, S. Zhu, Y. Li, and Y. Yin, "Passive MIMO radar detection with unknown colored Gaussian noise," *Remote Sens.*, vol. 13, no. 14, p. 2708, Jul. 2021.

[19] J. L. Garry, C. J. Baker, and G. E. Smith, "Evaluation of direct signal suppression for passive radar," *IEEE Trans. Geosci. Remote Sens.*, vol. 55, no. 7, pp. 3786–3799, Jul. 2017.

[20] Q. Wu, Y. D. Zhang, M. G. Amin, and B. Himed, "High-resolution passive SAR imaging exploiting structured Bayesian compressive sensing," *IEEE J. Sel. Topics Signal Process.*, vol. 9, no. 8, pp. 1484–1497, Dec. 2015.

[21] J. Yang, T. Jin, and X. Huang, "Compressed sensing radar imaging with magnitude sparse representation," *IEEE Access*, vol. 7, pp. 29722–29733, 2019.

[22] M. Li, X. Xi, X. Zhang, and G. Liu, "Joint compressed sensing and spread spectrum through-the-wall radar imaging," *IEEE Access*, vol. 9, pp. 6259–6267, 2021.

[23] J. Akhtar and K. E. Olsen, "Formation of range-Doppler maps based on sparse reconstruction," *IEEE Sensors J.*, vol. 16, no. 15, pp. 5921–5926, Aug. 2016.

[24] W. Feng, J.-M. Friedt, G. Cherniak, and M. Sato, "Batch compressive sensing for passive radar range-Doppler map generation," *IEEE Trans. Aerosp. Electron. Syst.*, vol. 55, no. 6, pp. 3090–3102, Dec. 2019.

[25] X. Zhang, J. Sward, H. Li, A. Jakobsson, and B. Himed, "A sparsity-based passive multistatic detector," *IEEE Trans. Aerosp. Electron. Syst.*, vol. 55, no. 6, pp. 3658–3666, Dec. 2019.

[26] J. H. G. Ender, "A compressive sensing approach to the fusion of PCL sensors," in *Proc. 21st EUSIPCO*, Sep. 2013, pp. 1–5.

[27] W. Ketpan and M. Sellathurai, "Compressive sensing-based 3D signal extraction for MIMO passive radar using OFDM waveforms," in *Proc. IEEE Int. Conf. Commun. (ICC)*, May 2016, pp. 1–6.

[28] B. Sun, H. Chen, X. Wei, and X. Li, "Multitarget direct localization using block sparse Bayesian learning in distributed MIMO radar," *Int. J. Antennas Propag.*, vol. 2015, May 2015, Art. no. e903902.

[29] A. Abtahi, S. Gazor, and F. Marvasti, "Off-grid localization in MIMO radars using sparsity," *IEEE Signal Process. Lett.*, vol. 25, no. 2, pp. 313–317, Feb. 2018.

[30] B. Li and A. Petropulu, "Efficient target estimation in distributed MIMO radar via the ADMM," in *Proc. 48th Annu. Conf. Inf. Sci. Syst. (CISS)*, Mar. 2014, pp. 1–5.

[31] H. Nikaein, A. Sheikhi, and S. Gazor, "Target detection in passive radar sensors using least angle regression," *IEEE Sensors J.*, vol. 21, no. 4, pp. 4533–4542, Feb. 2021.
[32] X. Lv, G. Bi, and C. Wan, "The group lasso for stable recovery of block-sparse signal representations," *IEEE Trans. Signal Process.*, vol. 59, no. 4, pp. 1371–1382, Apr. 2011.
[33] Y. C. Eldar, P. Kuppinger, and H. Bolcskei, "Block-sparse signals: Uncertainty relations and efficient recovery," *IEEE Trans. Signal Process.*, vol. 58, no. 6, pp. 3042–3054, Jun. 2010.
[34] X. Wang, W. Guo, Y. Lu, and W. Wang, "Distributed compressed sensing for block-sparse signals," in *Proc. IEEE 22nd Int. Symp. Pers., Indoor Mobile Radio Commun.*, Sep. 2011, pp. 695–699.
[35] G. Swirszcz, N. Abe, and A. C. Lozano, "Grouped orthogonal matching pursuit for variable selection and prediction," *Adv. Neural Inf. Process. Syst.*, vol. 22, pp. 1150–1158, 2009.
[36] Z. Ben-Haim and Y. C. Eldar, "Near-oracle performance of greedy block-sparse estimation techniques from noisy measurements," *IEEE J. Sel. Topics Signal Process.*, vol. 5, no. 5, pp. 1032–1047, Sep. 2011.
[37] C. Moscardini, D. Petri, A. Capria, M. Conti, M. Martorella, and F. Berizzi, "Batches algorithm for passive radar: A theoretical analysis," *IEEE Trans. Aerosp. Electron. Syst.*, vol. 51, no. 2, pp. 1475–1487, Apr. 2015.
[38] R. Nitzberg, *Radar Signal Processing and Adaptive Systems*. Norwood, MA, USA: Artech House, 1999.

HOSSEIN NIKAEIN received the B.Sc. degree in electronics engineering and the M.Sc. degree in control systems engineering from Isfahan University of Technology, Isfahan, Iran, in 1997 and 2001, respectively, and the Ph.D. degree in communication systems engineering from Shiraz University, Shiraz, Iran, in 2021. From September 2017 to August 2018, he was a Visiting Scholar with the Department of Electrical Engineering, Queen's University, Kingston, ON, Canada. His research interests include statistical signal processing, compressive sensing, and bioinformatics.

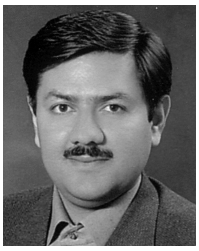

ABBAS SHEIKHI was born in Shiraz, Iran, in 1971. He received the B.Sc. degree in electronics engineering from Shiraz University, Shiraz, in 1993, and the M.Sc. degree (Hons.) in biomedical engineering and the Ph.D. degree (Hons.) in communications engineering from Sharif University of Technology, Tehran, Iran, in 1995 and 1999, respectively. Since 1999, he has been with the Department of Electrical and Electronics Engineering, Shiraz University, where he holds the position of a Professor. His current research interests include detection, estimation, and radar signal, and data processing.

SAEED GAZOR (Senior Member, IEEE) received the B.Sc. degree *(summa cum laude)* in electronics engineering and the M.Sc. degree *(summa cum laude)* in communication systems engineering from Isfahan University of Technology, in 1987 and 1989, respectively, and the Ph.D. degree in signal and image processing from the Département Signal Télecom ParisTech [formerly École Nationale Supérieure des Télécommunications (ENST)], Paris, France, in 1994. He was an Assistant Professor with the Department of Electrical and Computer Engineering, Isfahan University of Technology, from 1995 to 1998. He was a Research Associate with the University of Toronto, from 1999 to 1999. Since 1999, he has been a Faculty Member with Queen's University, Kingston, ON, Canada, where he is currently a Full Professor with the Department of Electrical and Computer Engineering and also cross-appointed to the Department of Mathematics and Statistics. His main research interests include statistical and adaptive signal processing, detection and estimation theory, cognitive signal processing, distributed array signal processing, speech processing, image processing, MIMO communication systems, collaborative networks, channel modeling, and information theory. He is a member of Professional Engineers Ontario. His research received a number of awards, including the Provincial Premier's Research Excellence Award, the Canadian Foundation of Innovation Award, the Ontario Innovation Trust Award, and the Intel Research Excellence Award. He has been on the technical program committee of numerous conferences and served as an organizing committee member for many international conferences in various capacities. He has served as an editor for several journals.